

Order-disorder transition induced by deformation of vortex lines at the twin boundaries in $\text{YBa}_2\text{Cu}_3\text{O}_{7-\delta}$ -crystals: test of the Lindemann criteria

Yu. T. Petrusenko

National Science Center "Kharkov Institute of Physics and Technology",
1 Akademicheskaya St., Kharkov 61108, Ukraine

A. V. Bondarenko,* A. A. Zavgorodniy, M. A. Obolenskii, and V. I. Beletskii

Physical department, V.N. Karazin Kharkov National University, 4 Svoboda Square, 61077 Kharkov, Ukraine

(Dated: November 1, 2018)

We show that rotation of the magnetic field off the plane of twin boundaries (TB's) induces transition of an ordered vortex solid phase to a disordered one. This transition arises due to appearance of transverse deformations of vortex lines near the

criteria, $u_{t,rp} = c_L a_0$. This order-disorder transition is accompanied by an increase in the depinning current, by crossover from an elastic creep to plastic one, and by appearance of the S -shaped voltage-current characteristics.

PACS numbers: 74.25.Qt, 74.25.Sv, 74.72.Bk

The non-monotonous field variation of the pinning force F_p in low- T_c (NbSe_2 [1, 2], V_3Si [3]) and high- T_c (BiSrCaCuO [4], YBaCuO [5, 6]) superconductors is subject of long-time interest. Increase of the pinning force can be explained by softening of the elastic moduli of vortex lattice in vicinity of the upper critical field $H_{c2}(T)$ [2] or the melting line $H_m(T)$ [7] that causes better adaptation of the vortex lines to the pinning landscape. In frames of the collective pinning theory [8] the non-monotonous field variation of the force F_p in the thermally activated mode is determined by competition between increase of the activation energy U and decrease of the depinning current J_d upon increase of the field. Two alternative models [9, 10] suggest transition of an ordered VL into a disordered one with increased magnetic field, though the nature of the order-disorder (OD) transition and increase of the force F_p in these models are different. These models are supported by correlation between the field corresponded to the structural OD

transition [11] and the onset of the F_p increase [4] in BiCaSrCuO crystals.

The model proposed in Ref. 13 assumes that OD transition occurs when transverse deformations of vortex lines $u_{t,rp}$, induced by interaction of vortices with random pinning potential, satisfy the Lindemann criteria, $u_{t,rp} = c_L a_0$, where $a_0 \simeq (\Phi_0/B)^{1/2}$ is the inter-vortex distance, Φ_0 is the flux quantum, and c_L is the Lindemann number. This model can be tested in the $\text{YBa}_2\text{Cu}_3\text{O}_{7-\delta}$ crystals through investigation of the effect of the magnetic field rotation off the TB's plane on pinning and dynamics of the vortex solid (VS). Indeed, decoration experiments [14] show that the superconducting order parameter at the TB's is suppressed. This causes deformation of the vortex lines near the TB's, as it is shown in Fig. 1a [12]. Here, at the angles $\theta \equiv \angle \mathbf{H}, \text{TB}$'s smaller than a certain critical θ_c value, a some part of the vortex line L_{TB} is trapped by the TB, the vortex fragment L_h and the twin plane limit the angle θ_c , and far away from the TB the vortex line is aligned along the external field. These deformations induce appearance of transverse displacements of the vortex line, the amplitude of which $u_{t,TB}$ can satisfy the Lindemann criteria in high magnetic field. Therefore, according to Ref. 13, one can expect occurrence of the OD transition when rotating the field off the TB's plane. Results of our measurements give strong experimental support for occurrence of this transition.

The measurements were performed on two $\text{YBa}_2\text{Cu}_3\text{O}_{7-\delta}$ crystals with $T_c \simeq 93$ K and $\delta T_c \simeq 0.4$ K, which contained TB's aligned in one direction. The transport current was applied along the ab -plane and at angle of 90° and 45° to the TB's plane in crystals C1 and C2, respectively. The average distance between the TB's was about $0.8 \mu\text{m}$ in sample C1, and about $0.3 \mu\text{m}$ in sample C2. Measurements were performed for different orientations of vector \mathbf{H} with respect to the c -axis. In sample C1 the vector \mathbf{H} was located in plane constituted by the vectors \mathbf{c} and \mathbf{J} , while in sample C2 it

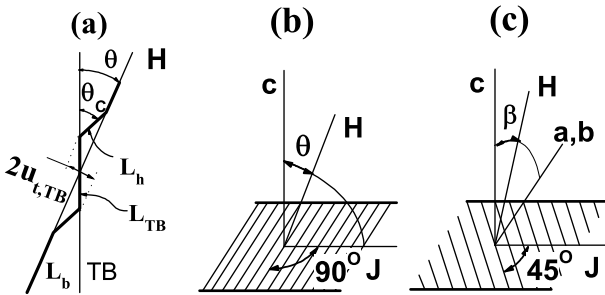


FIG. 1: Kinked structure of vortex line near the plane of TB proposed in Ref. 12 (panel a), and sketch of measurements geometry of crystal C1 (panel b) and C2 (panel c).

*Electronic address: Aleksandr.V.Bondarenko@univer.kharkov.ua

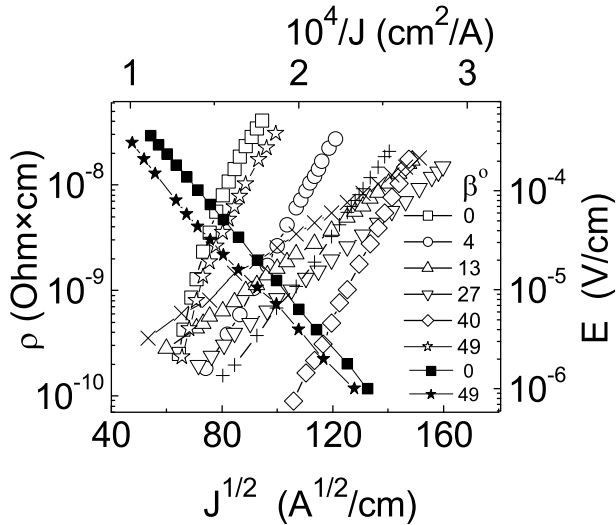


FIG. 2: The $E(J)$ curves in crystal C2, which are plotted in the scale $\log \rho = \log[E(J)/J]$ vs. \sqrt{J} (light symbols, left-hand and bottom scales), and in the scale $\log E(J)$ vs. $1/J$ (dark symbols, right-hand and top scales). Cross-wis symbols correspond to voltage-current characteristics plotted in the scale $\log \rho$ vs. \sqrt{J} , which were measured in the parallel field after electron irradiation with doses of 10^{18} (+) and $3 \cdot 10^{18}$ (x) el/cm². Irradiation dose 10^{18} produces the averaged over all sublattices concentration of the defects 10^{-4} dpa.

was located in plane perpendicular to the vector \mathbf{J} , as it is shown in panel (a) and (b) of Fig. 1, respectively. The resolution of angles θ and $\beta \equiv \angle \mathbf{H}, \mathbf{c}$ was about 0.1° . The concentration of point defects n_{pd} in sample C2 was varied by low-temperature ($T \leq 10$ K) irradiation with 2.5 MeV electrons, and the irradiation-measurements cycles were performed without heating the sample above 110 K [15]. The vortex dynamics was studied through measurements of current-voltage characteristics $E(J)$ at dc -current by the standart four-probe method at a temperature of $t \equiv T/T_c = 0.92$ in a magnetic field of 15 kOe.

The measurement results of sample C2, plotted as $\log E(J)$ versus $1/J$ and $\log \rho(J) \equiv \log E(J)/J$ versus \sqrt{J} , are shown in Fig. 2. The dynamic resistance $\rho_d(J) \equiv dE(J)/dJ$ corresponded to the measured $E(J)$ dependencies is much smaller than the flux flow resistance ρ_{BS} indicating that measurements correspond to the thermally activated creep mode. It is seen that in non irradiated sample and at angle β of $\beta = 0^\circ$ and $\beta = 49^\circ$ the experimental data follows equation

$$E(J) = e_0 \exp[-U_{el}/k_B T](J_d/J) \quad (1)$$

correspondent to the elastic mechanism of vortex creep [8], while in the interval of angles $4^\circ \leq \beta \leq 49^\circ$ they follows equation

$$E(J) = \rho_0 J \exp\{-U_{pl}/k_B T[1 - (J/J_d)^{0.5}]\} \quad (2)$$

which corresponds to the plastic creep mediated by motion of the VS dislocations. Here E_0 and ρ_0 are the con-

stants, and U_{el} and U_{pl} are the activation energies correspondent to elastic and plastic creep, respectively. It is also seen that in irradiated sample the creep follows Eq. 2 at angle β of $\beta = 0^\circ$. The crossover from elastic to plastic creep, realized in the field $\mathbf{H} \parallel \mathbf{c}$ with an increased concentration n_d , is caused by OD transition [15]. The transition arises due to increase in the pinning energy, $E_p \propto n_d^{1/3}$ [8], which dominates over increase of the elastic energy induced by transverse deformations $u_{t,rp} = c_L a_0$. The crossover from elastic to plastic creep, which is observed in a non irradiated sample at field rotation off the TB's plane through $\beta \geq 4^\circ$, can arise due to the OD transition, too. But in this case it is initiated by appearance of transverse displacements of vortex lines near the TB's, $u_{t,TB}$, see Fig. 1b. The displacement amplitude

$$u_{t,TB} \simeq L_h \sin(\theta_c - \theta) \quad (3)$$

is specified by the length of fragment $L_h \simeq (\varepsilon a_0 / 2\sqrt{\pi}) [\ln(a_0/\xi)]^{1/2}$ [12], and the angles β and θ in sample C2 are related by $\sqrt{2}\sin\theta = \sin\beta$. Decoration experiments [16] show that TB's affect vortex structure up to angle $\theta_c \simeq 70^\circ$, when the field is rotated off the c -axis. For $a_0(15\text{kOe}) = 400$ Å, $\theta = 4^\circ$, $\theta_c \simeq 70^\circ$, and for reasonable values of the anisotropy parameter $\varepsilon = 1/5$ and coherence length $\xi(85\text{K}) = 40$ Å we obtain the amplitude $u_t \simeq 0.1a_0$, which satisfy the Lindemann criteria.

The crossover from elastic to plastic creep is observed in the sample C1 too. In this sample, as evident from Fig. 3c, the value of ratio $\rho_d/\rho_{BS} \ll 1$ corresponds to the creep regime at small currents, while at high currents the ratio $\rho_d/\rho_{BS} \simeq 1$ corresponds to the flux flow regime. Angular variation of the critical currents J_{E1} and J_{E2} inside the creep regime (determined at voltage criteria of 2 and 100 $\mu\text{V}/\text{cm}$, respectively) and of the depinning current J_d (determined by extrapolation of the linear parts of the $E - J$ curves in zero voltage) is shown in Fig. 4a. The currents J_d and J_{E1} vary with the angle θ in a similar way: they gradually increase with angle θ up to the value of $\theta = 25^\circ$, and then sharp drop down to their values at angle $\theta = 0^\circ$. Fig. 4b shows angular variation of the critical currents J_{E1} and J_{E2} , determined at the same voltage criteria, in sample C2.

The rise in J_c , observed in the angular range $0 < \theta \leq 25^\circ$ can not be explained by enhanced pinning of the trapped fragments L_{TB} because their portion (the value of ratio L_{TB}/L_b) decreases as $\sin(\theta_c - \theta)$. Also, the reduced pinning in the field $\mathbf{H} \parallel \mathbf{c}$ can not be explained by suppression of pinning by point defects, as it was assumed in Ref. 17: the vortices located in between the TB's poorly accommodate themselves to the point defects landscape due to a strong interaction with vortices trapped by the TB's. This interpretation implies the formation of the ordered VS in the irradiated samples placed in the parallel field; that contradicts the results of our measurements. Therefore we believe that the current J_d increases due to occurrence of the OD transition. This interpretation implies that weak 1D-pinning

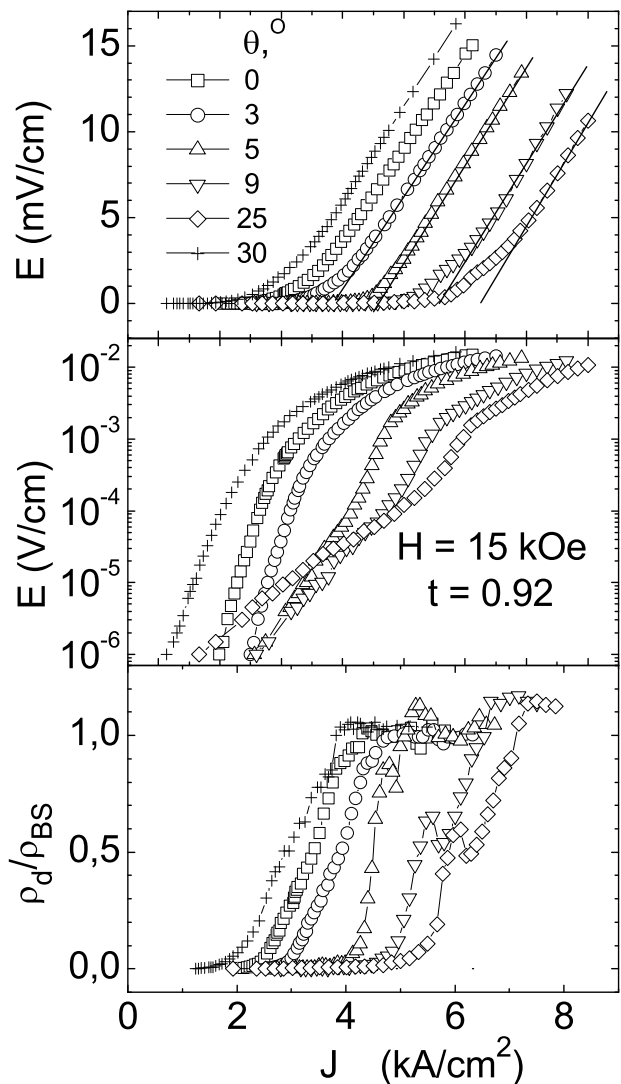


FIG. 3: The $E(J)$ curves in crystal C1 plotted in the linear (panel a) and semi-logarithmical (panel b) scale. Panel c shows the $\rho_d(J)/\rho_{BS}$ curves plotted in the linear scale.

of the ordered VS, which realizes in the parallel field, is replaced by strong 3D-pinning of the disordered VS in the inclined fields. Density of the displacements (number of displacements $n_{t,TB}$ per unit vortex length) increases as $n_{t,TB} \propto \sin\theta$, this leading to continuous increase of the dislocation concentration, and thus, to a greater disorder of the vortex solid. Therefore the current J_d increases due to better adaptation of the disordered phases to the pinning landscape [18] and [19]. On the other hand, according to Eq. 3 the amplitude $u_{t,TB}$ decreases with increased angle θ . Therefore, as soon as it drops below the value of $c_L a_0$, one can expect transformation of the disordered VS into the ordered VS. This transition must be accompanied by the crossover of the 3D to 1D pinning regime that reduces the pinning force, and by the crossover of the plastic to elastic creep regime. Sharp drop in the current J_c and crossover from the plastic to

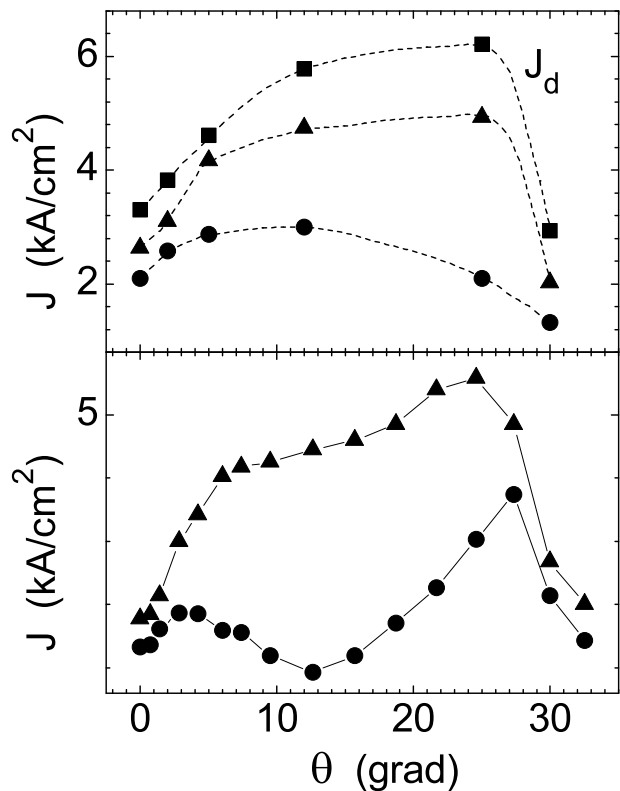


FIG. 4: Angular variation of the depinning current J_d (squares) and of the currents J_{E1} and J_{E2} determined at electric field level of $E_1 = 2 \mu\text{V}/\text{cm}$ (circles) and $E_2 = 100 \mu\text{V}/\text{cm}$ (triangles), respectively, in crystal C1 (panel a) and C2 (panel b).

elastic mechanism of vortex creep, which are realized in the narrow interval of angles $25^\circ \leq \beta \leq 30^\circ$, strongly support occurrence of this transition.

An important feature of vortex dynamics is that the resistance ρ_d monotonous increases with the current at angles $\theta = 0^\circ$ and $\theta = 30^\circ$, while in the interval of angles $5^\circ \leq \beta \leq 25^\circ$ a peak in the $\rho_d(J)$ curves is observed, see Fig. 3c. This peak corresponds to the S-shape of the $E(J)$ curves, which in some papers is attributed to possible non homogeneous distribution of the magnetic flux or current in samples. However, it is difficult to point out any reliable mechanism responsible for the change of homogeneity of these parameters with small change in the angle θ , namely, with its variation from 0 to 5° , or from 25° to 30° . Therefore we believe that the peak is dynamic characteristic of the disordered VS, and it characterizes the dynamic ordering of the VS in presence of the random pinning potential, as it is observed in the numerical studies [20, 21]. This ordering is caused by reduction in the amplitude $u_t \propto 1/v$ [22], and realizes in the interval of currents confined by the peak and minimum position in the $\rho_d(J)$ curves [20, 21]. The effect of dynamic ordering on the pinning of VS in $\text{YBa}_2\text{Cu}_3\text{O}_{7-\delta}$ crystals containing chaotic pinning potential has been recently studied in Ref. 23. It has been found that dynamic ordering sub-

stantially reduces the pinning force. Note that in crystal C1 vortices move along the plane of TB's and the amplitude $u_{t,TB}$ is not changed with v due to 2D nature of these defects. Therefore increase in v partially orders the VS, but dynamic VS remains disordered due to permanent amplitude $u_{t,TB}$ that causes substantial increase of the current J_d in the interval of angles $0 < \theta \leq 25^\circ$.

As seen in Fig. 4a, angular variation of the current J_{E1} , which characterizes pinning in deep creep regime, differs from the $J_d(\theta)$ and $J_{E2}(\theta)$ dependencies. This is reasonable considering that inside deep creep regime the pinning force depends on both the depinning current and activation energy. The activation energy correspondent to the plastic creep depends on the angle $\alpha \equiv \angle \mathbf{H}, ab$ [15] and amplitude $u_{t,TB}$ [24]. It can be shown that in presence of correlated displacements $u_{t,TB}$ the energy U_{pl} depends on mutual orientation of the displacements and direction of vortex motion. This is caused different angular variation of the current J_{E1} in samples C1 and C2. Detailed analysis of this difference and of the effect of

point disorder on angular variation of the energy U_{pl} and on angular variation of the currents J_{E1} and J_{E2} will be discussed elsewhere [25].

In conclusion, we have studied the effect of transverse deformation of vortex lines near the planes of TB's on the pinning force, mechanism of thermally activated creep, and dynamics of vortex solid. We show that in the interval of angles $5 \leq \theta \leq 25^\circ$ the amplitude of displacements $u_{t,TB}$ satisfy the Lindemann criteria, $u_{t,TB} = c_L a_0$, that leading to formation of the disordered vortex solid. This phase is characterized by the plastic creep mediated by motion of dislocations, by increase of the depinning current with increased density of the displacements, and by the S-shaped voltage-current characteristics, which manifests partial dynamic ordering of the vortex solid induced by suppression of the effect of random point pinning potential. Decrease of the amplitude $u_{t,TB}$ below the value of $c_L a_0$ causes transition to the ordered vortex solid, which is characterized by the elastic creep and smaller depinning current.

-
- [1] S. Bhattacharya and M. J. Higgins, Phys. Rev. Lett. **70**, 2617 (1993).
- [2] M. J. Higgins and S. Bhattacharya, Physica (Amsterdam) **C257**, 232 (1996).
- [3] A. A. Gapud, D. K. Christen, J. R. Thompson, and M. Yethiraj, Phys. Rev. B **67**, 104516 (2003).
- [4] B. Khaikovich, E. Zeldov, D. Majer, T. W. Li, P. H. Kes, and M. Konczykowski, Phys. Rev. Lett. **76**, 2555 (1996).
- [5] H. Kupfer, T. Wolf, A. Z. C. Lessing, X. Langon, R. Meier-Hirmer, W. Schauer, and H. Wuhl, Phys. Rev. B **58**, 2886 (1998).
- [6] M. Pissass, E. Moraitakis, G. Kallias, and A. Bondarenko, Phys. Rev. B **62**, 1446 (2000).
- [7] W. K. Kwok, J. A. Fendrich, C. J. van der Beek, and G. W. Crabtree, Phys. Rev. Lett. **73**, 2614 (1994).
- [8] G. Blatter, M. V. Feigel'man, V. B. Geshkenbein, A. I. Larkin, and V. M. Vinokur, Rev. Mod. Phys. **66**, 1125 (1994).
- [9] D. Ertas and D. Nelson, Physica C **272**, 79 (1996).
- [10] B. Rosenstein and V. Zhuravlev, Phys. Rev. B **76**, 014507 (2007).
- [11] R. Cubbit and et al., Nature(London) **365**, 407 (1993).
- [12] W. K. Kwok, J. A. Fendrich, V. M. Vinokur, A. E. Koshelev, and G. W. Crabtree, Phys. Rev. Lett. **76**, 4596 (1996).
- [13] D. Ertas and D. Nelson, Physica (Amsterdam) **C272**, 79 (1997).
- [14] L. Vinnikov, L. Gurevich, G. Yemelchenko, and Y. Osipyan, Solid St. Commun. **67**, 421 (1988).
- [15] A. V. Bondarenko, A. A. Prodan, M. A. Obolenskii, R. V. Vovk, and T. R. Arouri, Low Temp. Phys. **27**, 339 (2001), [Fizika Nizk. Temp. **27**, 463 (2001)].
- [16] J. Herbsommer, G. Nieva, and J. Luzuriaga, Phys. Rev. B **62**, 3534 (2000).
- [17] V. Solovjov, V. Pan, and H. Freyhardt, Phys. Rev. B **50**, 13724 (1994).
- [18] M. Gingras and D. Huse, Phys. Rev. B **53**, 15193 (1996).
- [19] T. Giamarchi and P. Le Doussal, Phys. Rev. B **55**, 6577 (1997).
- [20] M. C. Faleski, M. C. Marchetti, and A. A. Middleton, Phys. Rev. B **54**, 12427 (1996).
- [21] A. B. Kolton, D. Dominguez, and N. Grobech-Jensen, Phys. Rev. Lett. **83**, 3061 (1999).
- [22] A. Koshelev and V. Vinokur, Phys. Rev. Lett. **73**, 3580 (1994).
- [23] A. V. Bondarenko, A. Zavgorodniy, D. A. Lotnik, M. A. Obolenskii, R. V. Vovk, and Y. Biletskiy, arXiv:0803.0880v2 [cond-mat.supr-con] (2008).
- [24] A. V. Bondarenko, A. A. Prodan, Y. T. Petrusenko, V. N. Borisenko, F. Dworschak, and U. Dedek, Phys. Rev. B **64**, 092513 (2001).
- [25] A. V. Bondarenko and Y. T. Petrusenko, to be published (2008).